Journal of Magnetic Resonance 238 (2014) 1–7

Contents lists available at ScienceDirect

Journal of Magnetic Resonance

journal homepage: www.elsevier.com/locate/jmr

Coupled modes, frequencies and fields of a dielectric resonator and a cavity using coupled mode theory

Sameh Y. Elnaggar [a], Richard Tervo [a], Saba M. Mattar [b,*]

[a] Department of Electrical and Computer Engineering, University of New Brunswick, Fredericton, New Brunswick E3B 6E2, Canada
[b] Department of Chemistry and Centre for Laser, Atomic and Molecular Sciences, University of New Brunswick, Fredericton, New Brunswick E3B 6E2, Canada

ARTICLE INFO

Article history:
Received 2 August 2013
Revised 24 October 2013
Available online 6 November 2013

Keywords:
Electron paramagnetic resonance
Dielectric resonators
Resonance cavity
Resonator modes
Coupled mode theory
Coupled modes
Resonator frequency
Finite element methods
Magnetic field distributions
Electric field distributions
Filling factor
Spectrometer sensitivity
Signal-to-noise ratio

ABSTRACT

Probes consisting of a dielectric resonator (DR) inserted in a cavity are important integral components of electron paramagnetic resonance (EPR) spectrometers because of their high signal-to-noise ratio. This article studies the behavior of this system, based on the coupling between its dielectric and cavity modes. Coupled-mode theory (CMT) is used to determine the frequencies and electromagnetic fields of this coupled system. General expressions for the frequencies and field distributions are derived for both the resulting symmetric and anti-symmetric modes. These expressions are applicable to a wide range of frequencies (from MHz to THz). The coupling of cavities and DRs of various sizes and their resonant frequencies are studied in detail. Since the DR is situated within the cavity then the coupling between them is strong. In some cases the coupling coefficient, κ, is found to be as high as 0.4 even though the frequency difference between the uncoupled modes is large. This is directly attributed to the strong overlap between the fields of the uncoupled DR and cavity modes. In most cases, this improves the signal to noise ratio of the spectrometer. When the DR and the cavity have the same frequency, the coupled electromagnetic fields are found to contain equal contributions from the fields of the two uncoupled modes. This situation is ideal for the excitation of the probe through an iris on the cavity wall. To verify and validate the results, finite element simulations are carried out. This is achieved by simulating the coupling between a cylindrical cavity's TE_{011} and the dielectric insert's $TE_{01\delta}$ modes. Coupling between the modes of higher order is also investigated and discussed. Based on CMT, closed form expressions for the fields of the coupled system are proposed. These expressions are crucial in the analysis of the probe's performance.

1. Introduction

The coupling between a dielectric resonator (DR) and a conducting cavity is of interest in electron paramagnetic resonance (EPR) spectroscopy because of the signal to noise ratio (SNR) enhancement of the resulting probe [1–4]. When both resonators have the same resonance frequency, the size of the DR is much smaller than that of the cavity. Therefore the magnetic field of the DR is more concentrated in a much smaller spatial region. This leads to an increase in the resonator's filling factor [4]. Usually the frequency of the dielectric $TE_{01\delta}$ mode and that of the rectangular cavity's TE_{102} mode (TE_{011} mode for cylindrical cavities) are close. Two DRs inserted in a cavity allow the user to tune the frequency of the cavity along with enhancing the SNR [3,5,6].

The coupling between the $TE_{01\delta}$ DR mode and the cavity's TE_{011} mode was studied by Mett et al. [7]. They showed that the coupling could be modeled by lumped circuit (LC) elements. Using the LC model, crucial probe parameters such as frequencies, quality factors and resonator efficiencies were determined. The interaction of the dielectric and cavity modes results in two new modes. A symmetric (parallel) and an anti-symmetric (anti parallel) mode [7]. The symmetric mode is the mode formed when the two electromagnetic fields add constructively in phase, while the anti-symmetric mode has a 180° phase shift between the two uncoupled modes.

Using finite element simulations, the current authors showed that the interaction between the $TE_{01\delta}$ modes of two DRs and a TE_{102} cavity mode results in three coupled modes, where the most appropriate mode for X-band EPR experiments was found to be the TE^{+++} mode [6]. This mode is the result of the in-phase coupling of the three uncoupled ones (the two $TE_{01\delta}$ Dielectric modes and the TE_{102} cavity mode). In fact, it was illustrated that the fields of the TE^{+++} mode is the linear superposition of the three uncoupled ones [6]. The TE^{+--} mode does not have a cavity contribution. Accordingly, this mode is very difficult to excite through the cavity iris. As noted, the behavior of the coupled modes varies significantly. Thus for EPR experiments one needs to have a comprehensive

* Corresponding author. Fax: +1 506 453 4981.
E-mail address: mattar@unb.ca (S.M. Mattar).

1090-7807/$ - see front matter © 2013 Elsevier Inc. All rights reserved.
http://dx.doi.org/10.1016/j.jmr.2013.10.016

understanding of the modes' characteristics, particularly their frequencies and field distributions. Other field dependent parameters are of interest as well. Accordingly, the aim of the current paper is to thoroughly study the interaction of the modes of a single DR and an enclosing cavity. Coupled frequencies as well as field distributions are analytically determined.

Generally, coupled mode theory (CMT) is used to analyze and predict the behavior of a compound system by using the known properties of its simpler components. CMT can be divided into two main branches [8]. Space-coupled mode theory is useful in studying the properties of transmission systems such as waveguides and fiber optical systems. On the other hand, temporal-coupled mode theory is crucial in understanding the interaction between multiple resonators and is therefore suitable for the current work.

Usually CMT is applied to determine the frequencies (eigenvalues) of the coupled system. In the current manuscript, this step is taken further by calculating the coupled fields (eigenvectors) too. This is achieved by formulating the coupled mode equations from the first principles, i.e. from Maxwell's equations. By knowing the coupled frequencies and the fields of the coupled systems, a better understanding of probes with inserts can be achieved. Therefore, in this article, general expressions for the eigenvalues (frequencies) and the eigenvectors (fields) are calculated. The case when both resonators have the same uncoupled frequency (degenerate) is studied in detail. Other situations when the frequencies of the two subsystems are not the same are also thoroughly investigated. The results predicted by the coupled mode theory are compared to those of an electromagnetic (EM) full-wave numerical finite element simulator as well as to those found in the literature [7–9].

Section 2 defines the system and problem in a concise sense where the notations and the electric fields are presented. The eigenvalues and eigenvectors are derived in Section 3. This constitutes the main core needed to study the coupled system. Section 4 investigates and discusses the results obtained for different cases. The results are verified using finite element simulation. Summary and conclusions are presented in Section 5.

2. Theoretical background

The system under consideration is shown in Fig. 1. It consists of a DR, referred to as "1", inserted in the center of a cylindrical cavity, referred to as "2". The holder, not shown in the figure, is of a low loss/low permittivity material so its effect is negligible. Two types of DRs with vastly different dielectric constants were used. The first, labeled *type I, with* $\varepsilon_r = 29.2$, $d_1 = 6$ *mm*, $l_1 = 2.65$ *mm and* $f \approx 9.7$ GHz. The second labeled, *type II*, with $\varepsilon_r = 261$ $d_1 = 1.75$ mm, $l_1 = 1.75$ mm and $f \approx 9.5$ GHz. The terms d and l are the resonators diameter and height respectively. The cavity has an aspect ratio of $d_2/l_2 = 1$.

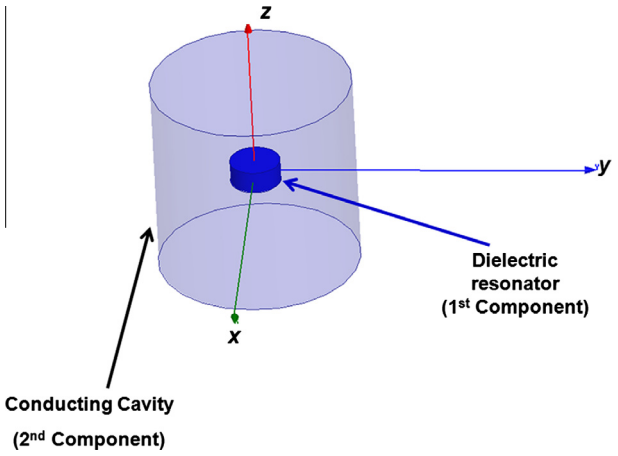

Fig. 1. System consisting of a DR inserted in a conducting cavity. The dielectric insert is held inside a hollow low loss/low permittivity holder (not shown).

The two uncoupled modes of interest are the dielectric $TE_{01\delta}$ mode and the cavity TE_{011} mode. The electric field of each mode can be written as [10],

$$E_{\varphi 1} = M_1 J_1(k_1 r) \begin{cases} \cos(\beta z) & r \leqslant \frac{d_1}{2},\ |z| \leqslant \frac{l_1}{2} \\ e^{\frac{\alpha l_1}{2}} \cos\left(\frac{\beta l_1}{2}\right) e^{-\alpha|z|} & r < \frac{d_1}{2},\ |z| > \frac{l_1}{2} \end{cases} \tag{1}$$

and

$$E_{\varphi 2} = M_2 J_1(k_2 r) \cos\left(\frac{\pi z}{d_2}\right). \tag{2}$$

Here k_1, k_2 are the dielectric and cavity radial wave numbers respectively. The symbol β is the wave number inside the dielectric in the z direction, $M_{1,2}$ are the fields' amplitudes and $E_{\varphi i}$ is the azimuthal electric field component. In deriving Eq. (1) a perfectly magnetic waveguide was assumed [11]. In addition, $k_1 = p_{01}/r_1$, where $p_{01} = 2.405$ and is the root of the 0th order Bessel function, $J_0(x)$. The symbol α is the attenuation factor, in the z direction, outside the DR resonator.

The magnetic field, which is the primary quantity that identifies the performance of the probe, can be determined from the electric field using Maxwell's equations, i.e.

$$\mathbf{H} = -\frac{1}{j\omega\mu_0} \nabla \times \mathbf{E},$$

where μ_0 is the permeability of free space and ω is the resonant frequency.

3. Theory

3.1. Derivation of the frequencies and fields by CMT

Using CMT, the fields of the coupled system are expressed as linear superposition of the uncoupled ones,

$$\mathbf{E} = a_1 \mathbf{E}_1 + a_2 \mathbf{E}_2, \tag{3}$$

$$\mathbf{H} = b_1 \mathbf{H}_1 + b_2 \mathbf{H}_2, \tag{4}$$

The isolated mode of the DR satisfies Maxwell's curl equations,

$$\nabla \times \mathbf{E}_1 = -j\omega_1 \mu_0 \mathbf{H}_1, \tag{5}$$

$$\nabla \times \mathbf{H}_1 = j\omega_1 \varepsilon_1 \mathbf{E}_1,$$

where

$$\varepsilon_1 = \begin{cases} \varepsilon_r \varepsilon_0 & \text{inside the dielectric material} \\ \varepsilon_0 & \text{otherwise.} \end{cases}$$

It incorporates the spatial variation due to the DR. The ω_1 symbol is the dielectric mode angular frequency. The variables $\mathbf{E}_1$ and $\mathbf{H}_1$ are the electric and magnetic fields respectively. Similarly, the cavity mode satisfies

$$\nabla \times \mathbf{E}_2 = -j\omega_2 \mu_0 \mathbf{H}_2 \tag{6}$$

and

$$\nabla \times \mathbf{H}_2 = j\omega_2 \varepsilon_2 \mathbf{E}_2,$$

where $\varepsilon_2 = \varepsilon_0$ is the permittivity of free space.

For the coupled system the curl equations are written as

$$\nabla \times \mathbf{E} = -j\omega\mu_0\mathbf{H}$$

and

$$\nabla \times \mathbf{H} = j\omega\varepsilon\mathbf{E} \tag{7}$$

Here ε is the permittivity of the coupled system. In this particular case

$$\varepsilon = \varepsilon_1 \tag{8}$$

By substituting Eqs. (3) and (4) in $\nabla \cdot (\mathbf{E}_i^* \times \mathbf{H})$, where ($i$ = 1, 2), and using identities Eqs. (5)–(7) one can find after integrating over the cavity volume

$$\sum_k \omega_i(C_{ik} + jM_{ik} - jS_{ik})b_k - \omega A_{ik}a_k = 0, \tag{9}$$

where

$$C_{ik} = \int_V \mu_0\mathbf{H}_i^* \cdot \mathbf{H}_k dV,$$

$$M_{ik} = \oint_{\partial V} \mathbf{E}_i^* \times \mathbf{H}_k \cdot d\vec{\mathbf{S}},$$

$$S_{ik} = -\oint_{\partial V} \mathbf{E}_i^* \times \mathbf{H}_k \cdot d\mathbf{S}$$

and

$$A_{ik} = \int_V \varepsilon\mathbf{E}_i \cdot \mathbf{E}_k dV$$

Since the tangential component of the electric field of the uncoupled cavity mode vanishes on the surface, then $M_{2k} = S_{2k} = 0$.

Similarly, by expanding $\nabla \cdot (\mathbf{E} \times \mathbf{H}_k^*)$ in terms of the uncoupled fields and integrating, one finds that

$$\sum_k [-\omega C_{ik}b_k + \omega_i D_{ik}a_k] = 0, \tag{10}$$

where $D_{ik} = \int_V \varepsilon_i \mathbf{E}_i^* \cdot \mathbf{E}_k dV$. Using Eq. (8) then

$$A_{1k} = D_{1k}$$

By integrating $\nabla \cdot (\mathbf{E}_i^* \times \mathbf{H}_k)$ over the cavity, the C_{ik} and D_{ik} terms can be related as

$$\omega_2 C_{21} = \omega_1 D_{12}^* \tag{11}$$

and

$$M_{12} = j\omega_1 C_{12} - j\omega_2 D_{21}^*. \tag{12}$$

The coupled modes can be then obtained by using Eqs. (9)–(12) and solving an eigenvalue problem. It is approximated by

$$\begin{bmatrix} \omega_1^2 & -\frac{\omega_2^2(\zeta_{12})}{A_{11}} \\ \frac{-\omega_1^2\zeta_{12} + (\omega_2^2 - \omega_1^2)D_{21}}{A_{22}} & \omega_2^2 \end{bmatrix} \begin{bmatrix} a_1 \\ a_2 \end{bmatrix} = \omega^2 \begin{bmatrix} a_1 \\ a_2 \end{bmatrix}, \tag{13}$$

where

$$\zeta_{12} = \varepsilon_0(\varepsilon_r - 1)\int_{DR} \mathbf{E}_1^* \cdot \mathbf{E}_2 dv \tag{14}$$

Here ζ_{12} is the overlap integral between the DR and CV. When the two resonators have the same resonant frequency, $\omega_1 = \omega_2 = \omega_0$, Eq. (13) reduces to

$$\begin{bmatrix} \omega_0^2 & \frac{-\omega_0^2\zeta_{12}}{A_{11}} \\ \frac{-\omega_0^2\zeta_{12}}{A_{22}} & \omega_0^2 \end{bmatrix} \begin{bmatrix} a_1 \\ a_2 \end{bmatrix} = \omega^2 \begin{bmatrix} a_1 \\ a_2 \end{bmatrix} \tag{15}$$

and by solving Eq. (15) the eigenvalues are found to be

$$\omega^2 = \omega_0^2\left(1 \pm \frac{\zeta_{12}}{\sqrt{A_{11}A_{22}}}\right)$$

Therefore the coupling coefficient is given by

$$\kappa = \frac{\zeta_{12}}{\sqrt{A_{11}A_{22}}} \tag{16}$$

Eq. (16) illustrates that the coupling coefficient depends on the overlap integral given by Eq. (14). It is also proportional to the interaction energy of the dielectric polarization vector, $\mathbf{P}_1 = (\varepsilon_r - 1)\varepsilon_0\mathbf{E}_1$, with the cavity field $\mathbf{E}_2$. Although the coupling coefficient, shown by Eq. (16), is expressed in terms of the overlap integral, ζ_{12}, the cavity still affects the DR by the surface current flowing on its wall, $\mathbf{J}_2$. Indeed, using properties Eqs. (12) and (11) one can deduce that (assuming that the system is lossless)

$$\zeta_{12} = \frac{T}{2\pi}\oint_{\partial V} \mathbf{E}_1^* \cdot \mathbf{J}_2 dV$$

For the general case, when $\omega_1 \neq \omega_2$, and assuming that the two frequencies are close enough such that $(\omega_2^2 - \omega_1^2)D_{21} \gg \omega_1^2\eta_{12}$, the symmetric and antisymmetric frequencies are found to be

$$(\omega^{++})^2 = \frac{\omega_1^2 + \omega_2^2}{2} - \sqrt{\left(\frac{\omega_1^2 - \omega_2^2}{2}\right)^2 + \omega_1^2\omega_2^2\kappa^2} \tag{17}$$

and

$$(\omega^{+-})^2 = \frac{\omega_1^2 + \omega_2^2}{2} + \sqrt{\left(\frac{\omega_1^2 - \omega_2^2}{2}\right)^2 + \omega_1^2\omega_2^2\kappa^2} \tag{18}$$

respectively. It is worth mentioning that Eqs. (17) and (18) depict a situation similar to that produced by perturbation theory in quantum mechanics [8].Solving the eigenvalue Eq. (13) the eigenvectors, **a**, are

$$a_2^{++} = \left(\frac{1}{2\kappa}(\gamma^2 - 1) + \sqrt{\frac{1}{4\kappa^2}(\gamma^2 - 1)^2 + \gamma^2}\right)a_1^{++} \tag{19}$$

for the symmetric mode and

$$a_2^{+-} = \left(\frac{1}{2\kappa}(\gamma^2 - 1) - \sqrt{\frac{1}{4\kappa^2}(\gamma^2 - 1)^2 + \gamma^2}\right)a_1^{+-} \tag{20}$$

for the anti-symmetric mode. Here γ^2 is equal to

$$\gamma^2 = \left(\frac{\omega_1}{\omega_2}\right)^2$$

The above general expressions are applicable to a wide range of frequencies (from MHz to THz).

4. Results and discussions

4.1. Eigenvalues and frequencies

To check the validity of the CMT analysis, the eigenvalue Eq. (13) is solved for a DR of *type I* by the Maple 13™ suite of programs (MapleSoft, a subsidiary of Cybernet Systems Co. Ltd.). The diameter of the cavity is allowed to change from 2.5 to 5.5 cm with a step of 1 mm, where d_2 is kept equal to l_2. The resulting frequencies are plotted and compared to the simulated ones using the eigenmodes solver in HFSS® (Ansys Corporation, Pittsburgh, PA, USA) as shown in Fig. 2. The HFSS program uses finite element methods to numerically solve for the electromagnetic fields and frequencies subjected to the boundary conditions. For our simulations, the losses did not significantly affect the results. The relative frequency

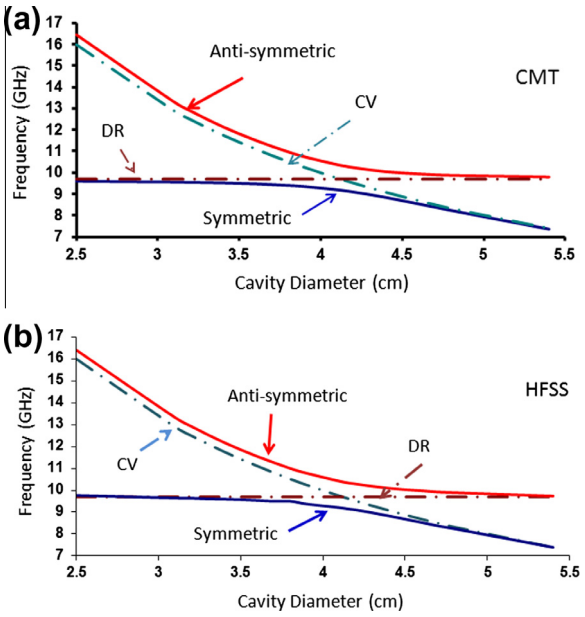

Fig. 2. Frequency of the symmetric and anti-symmetric modes due to the interaction of the DR ($\varepsilon_r = 29.2$, $d_1 = 6$ mm, $l_1 = 2.65$ mm) with the cavity ($d_2 = l_2$). (a) Using CMT and (b) using HFSS.

tolerance was taken to less be than 0.1%. The resulting figure shows that there is an excellent agreement between the frequencies obtained by the CMT and HFSS® methods.

Normally for a probe consisting of a DR in a small cavity (shield), one considers the frequency shifts of the modes to be minor. In general, HFSS computations only give a numerical value for the frequency. However, the analytical expression (17) derived by CMT gives more insight. It shows that the frequency is dependent on the coupling coefficient, κ. In the case of the anti-symmetric mode the deviation of the frequency from the uncoupled structures could be quite significant. Indeed the coupling coefficient is the normalized overlap integral, as suggested by Eqs. (14) and (16). Eq. (14) shows that as the cavity diameter decreases, $\mathbf{E}_1^* \cdot \mathbf{E}_2$ and the overlap integral increase. This leads to a larger coupling coefficient. Thus for small cavities, the term $\omega_1\omega_2\kappa$ in Eq. (17) is comparable to the term $(\omega_1^2 - \omega_2^2)/2$ and thus cannot be ignored. Hence the frequencies differ from the uncoupled frequencies, ω_1 and ω_2. For example, a cavity with $d_2 = 2.5$ cm its TE_{011} mode has a frequency of approximately 15.9 GHz. However, the frequency of the anti-symmetric mode of the coupled system is approximately 16.4 GHz. This 500 MHz shift is due to the increase in κ.

4.2. Eigenvectors

The behavior of the eigenvectors can be determined using Eqs. (19) and (20). When the two resonators are degenerate ($\gamma^2 = 1$), the eigenvectors for the symmetric mode reduce to

$$a_1 = a_2 \tag{21}$$

and for the anti-symmetric mode

$$a_1 = -a_2. \tag{22}$$

Eqs. (21) and (22) illustrate that the coupled modes contain equal contributions from the two uncoupled ones. One should expect that if the electric field of the coupled system is the vector sum of the electric fields of the uncoupled subsystems, as given by Eq. (3), then the radial variation of the magnitude of the electrical field will be the sum of the two Bessel functions presented in Eqs. (1) and (2). To verify the results of Eqs. (21) and (22), the magnitude of the electric fields for both the symmetric and anti-symmetric modes are calculated, using HFSS® as a 3D finite element solver, and plotted along the cavity radius in Fig. 3. In this case a DR of *type II* is used, while the cavity's diameter is equal to 4.1598 cm. These dimensions guarantee that the DR and cavity have the same resonant uncoupled frequencies of 9.5 GHz.

As observed from Fig. 3, the two modes have two peaks that correspond to the two Bessel functions in Eqs. (1) and (2). Indeed, the first peak is sharp and approximately occurs at the maximum of the uncoupled $TE_{01\delta}$ mode ($r = r_1 = 0.875$ mm) and the second one occurs at the cylindrical cavity's TE_{011} maximum point. This confirms that when the two modes have the same uncoupled frequencies, the coupled system contains a contribution from each mode.

Moreover, Fig. 3 shows that for the symmetric mode the electric has an appreciable value in the range of 0.0–5.0 mm. On the contrary, the electric field of the anti-symmetric mode has a node-like behavior in the same region. This is due to the negative sign in Eq. (22).

The filling factor is an important parameter because it directly affects the spectrometer's sensitivity. It depends on the magnetic field values at the sample compared to the total magnetic field in the whole probe. The magnetic fields of the coupled system are obtained from Eq. (10) by calculating the b_i coefficients in terms of the a_i coefficients. When the overlap integral is small, $b_i \approx a_i$. To further assess the magnetic fields' behavior of the coupled system, the variation of the magnetic field intensity along the cavity axis for the CV, DR and their coupled symmetric and anti-symmetric modes are illustrated in Fig. 4.

For a DR in free space the magnetic field is highly localized and is the largest. It is followed by the symmetric and anti-symmetric modes respectively. The uncoupled CV field is the smallest, is highly delocalized and spans one half wave length. This means the filling factors of the symmetric and anti-symmetric modes are substantially high but less than that of the DR in free space. Fig. 4 also shows that due to the cavity component, the magnetic fields of the coupled modes are significant in the region outside of the DR given by ($|z| > l_1/2$). This implies that the coupled modes can be easily excited through an iris or a loop positioned a quarter

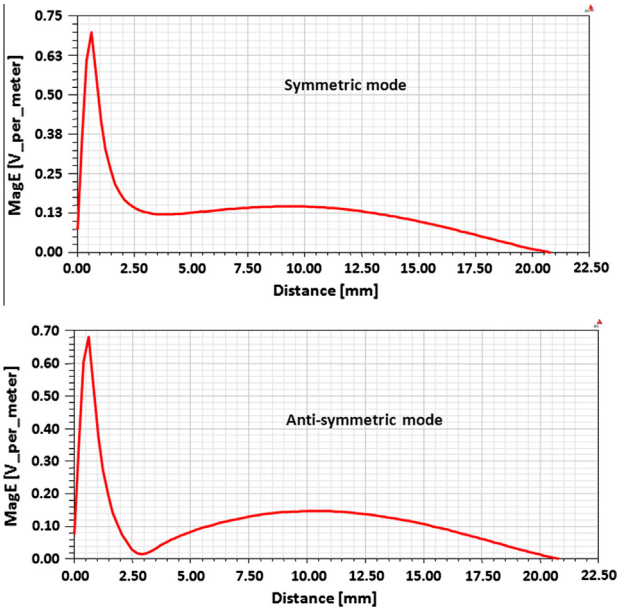

Fig. 3. The magnitude of the electric field of the coupled system plotted against the cavity radius.

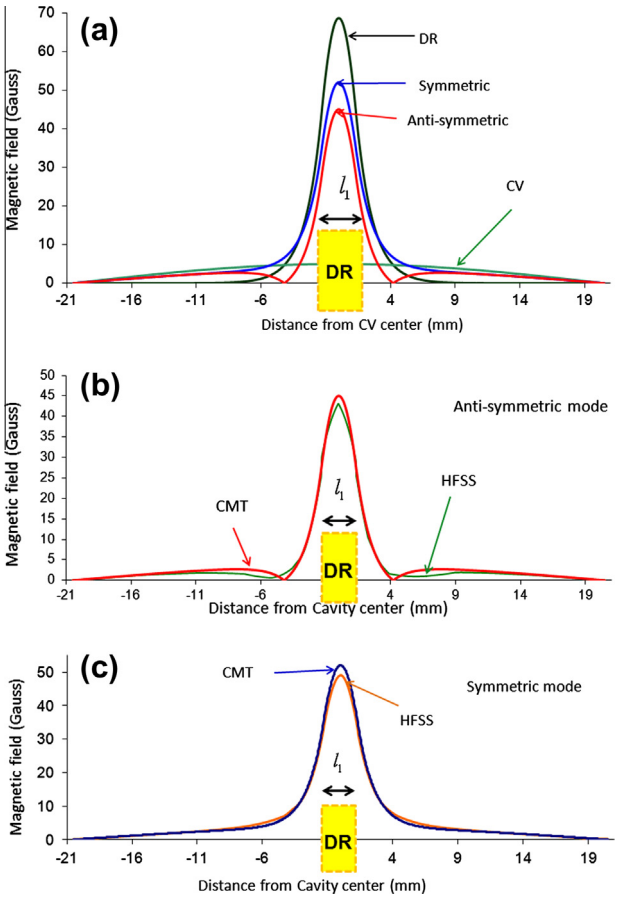

Fig. 4. Calculated magnetic fields along the cavity axis. (a) For the DR, CV (green online), symmetric (blue online) and anti-symmetric (red online) modes calculated using CMT. b) The anti-symmetric mode using CMT (red online) compared to HFSS® (green online). (c) The symmetric mode using CMT (blue online) compared to HFSS® (orange online). (For interpretation of the references to color in this figure legend, the reader is referred to the web version of this article.)

wavelength away from the center of the cavity upper, or side walls. The minima of the magnetic field of the anti-symmetric mode predicted by CMT in Fig 4b (red curve online) occurs closer to the center from that calculated by HFSS® (green curve online). This can be attributed to the fact that the field calculated using CMT relies on the Cohn model given by Eq. (1) which assumes that the DR is placed in a tight waveguide with perfectly magnetic walls.

In summary, this section demonstrates that the CMT used in the current article can find field values and give a clear picture of their distribution in probes.

The behavior of the cavity size on the probe's coupled modes is studied next. For a large cavity ($\omega_1 > \omega_2$), the limiting condition, $\gamma^2 \to \infty$, can be used. Consequently the overlap integral decreases, $\kappa \to 0$ and Eqs. (19) and (20) reduce to

$$a_2^{++} = 1, \quad a_1^{++} = 0 \tag{23}$$

$$a_1^{+-} = 1, \quad a_2^{+-} = 0 \tag{24}$$

Eqs. (23) and (24) imply that the two modes tend to decouple when the cavity's dimensions increase. This is of no surprise since the coupled energy due to the cavity surface current ($\mathbf{J}_2$) and the dielectric polarization vector ($\mathbf{P}_1$) have a smaller influence when the cavity dimensions increase.

However when the cavity shrinks, the situation gets more involved. In the limiting case when $\gamma^2 \to 0$, κ increases. Eqs. (19) and (20) then become,

$$a_1^{++} = 1, \quad a_2^{++} = 0 \tag{25}$$

$$a_1^{+-} = \frac{\kappa}{\sqrt{1+\kappa^2}}, \quad a_2^{+-} = -\frac{1}{\sqrt{1+\kappa^2}}. \tag{26}$$

Eq. (25) suggests that for small cavities, the symmetric mode tends to the dielectric mode. Thus the influence of the cavity on the frequencies and fields is minimal and it is considered a shield. These minute second order frequency changes are due to κ and the coupled induced frequency shifts [12].

For the anti-symmetric mode, in Eq. (26), the two field components from the cavity and dielectric are present. Thus even though the two modes have different frequencies, the coupled system still has contributions from both because κ is considerably large. A typical value for the coupling constant in such cases is between 0.4 and 0.5. To numerically verify the findings of Eq. (26), the DR of *type I* is inserted in a cavity with a frequency of 16.5 GHz ($\gamma^2 \approx 1/3$) and the electric field is simulated using HFSS®. The results are shown in Fig. 5.

Fig. 5 clearly shows that for small cavities, the anti-symmetric mode is a mix of the two fields. Indeed as seen from the figure and for small values of r, the fields' values are predominantly DR. However as r increases and because the cavity fields oppose that of the DR, the fields get diminishingly small in the vicinity of the arrow head in Fig. 5. For larger radius values, the fields' direction changes which is a clear indication that this mode is anti-symmetric. Moreover in this region the fields are predominately cavity-like. It is interesting to show that for such a case, the eigenvalue Eq. (13) can be solved to find the total electric field for the modes of the coupled system. In this case, the $a_{1,2}$ and $b_{1,2}$ are found to be $a_1 \approx b_1 = 0.41$ and $a_2 \approx b_2 = -0.92$. Therefore using Eq. (3), the electric and magnetic fields of the coupled anti-symmetric mode are equal to

$$\mathbf{E} = 0.41\mathbf{E}_1 - 0.92\mathbf{E}_2 \tag{27}$$

and

$$\mathbf{H} = 0.41\mathbf{H}_1 - 0.92\mathbf{H}_2 \tag{28}$$

This proves that there is a significant contribution from both resonators. The DR component localizes the magnetic field. Therefore the filling factor and the signal to noise ratio of the spectrometer are improved.

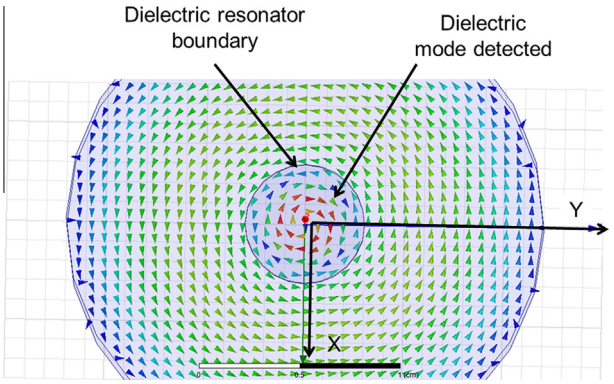

Fig. 5. The electric field of the anti-symmetric mode when the cavity is small (2.4 cm × 2.4 cm). Note the change in the direction of the field in the vicinity of the arrow.

Up to this point, we have considered the specific asymptotic cases when $\gamma^2 \to 0$ and $\gamma^2 \to \infty$. Next the behavior of the eigenvectors is calculated for various cavity dimensions (i.e. different γ^2 values).

Fig. 6 depicts the ratio a_2/a_1 for a range of cavity diameters (d_2 = 2.5–5.4 cm). Starting with a small cavity, the symmetric mode is predominantly DR in nature and is practically decoupled from the cavity. The cavity in this case is considered as a shield. On the other hand, the anti-symmetric mode is a mix of the two components. As the cavity dimensions increase, the symmetric mode gains TE_{011} character. On further increase it rapidly decouples and becomes cavity-like. This is clearly observed when its diameter is greater than 4.4 cm. For the anti-symmetric mode, the cavity decouples from the DR and the mode becomes DR-like in nature.

4.3. Coupling of a shield with higher DR modes

When $\omega_1^2 \gg \omega_2^2$, i.e. $\gamma^2 \gg 1$, the coupling between the cavity TE_{011} mode and the other dielectric higher modes, for example the $TE_{02\delta}$, is small. This is because the eigenvectors are given by Eqs. (23) and (24) where the two modes decouple. Another reason is that for small values of r, the radial component of cavity fields given by Eq. (2) inside the dielectric material can be approximated as [13]

$$J_1(k_c r) \approx \frac{k_c r}{2}$$

For instance, the radial component of the overlap integral of the cavity TE_{011} and the $TE_{02\delta}$ dielectric modes, is proportional to

$$\int_0^{r_d} J_1(k_c r)\cdot J_1(k_d r)dr \approx \int_0^{r_d} \frac{k_c r}{2}\cdot J_1(k_d r)dr. \tag{29}$$

Since for higher order dielectric modes, $J_1(k_d r)$ changes sign over the dielectric insert radius, the integration in Eq. (29) is small which leads to a small κ.

When the cavity dimension is decreased to the limit where the frequency of one of the higher dielectric modes (e.g. the $TE_{02\delta}$ mode) is close to the cavity TE_{011} mode then $\omega_1^2 \approx \omega_2^2$ ($\gamma^2 \approx 1$), and coupling is observed. For example, if the cavity's diameter is decreased down to 2.0 cm, its TE_{011} frequency $f_{TE_{011}} \approx 20$ GHz, which is close to the $TE_{02\delta}$ frequency, estimated to be ≈ 22 GHz. Therefore, the resulting coupled mode has a $TE_{02\delta}$ component as shown in Fig. 7. Here, one can see that inside the DR the field direction changes. This observation indicates that, inside the DR, the mode is predominantly $TE_{02\delta}$. Similarly at the region outside the DR, the mode is predominantly TE_{011}.

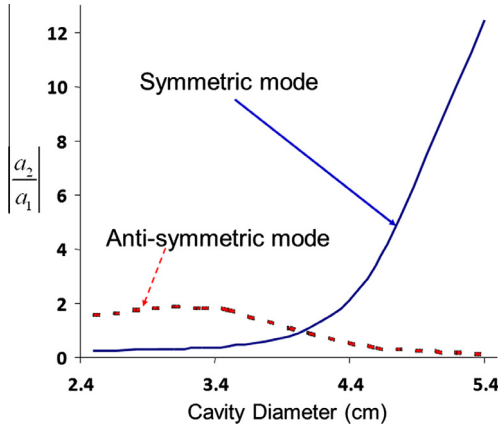

Fig. 6. The ratio $|a_2/a_1|$ which is an indication of how the fields decouple. When it is small the mode is more like a dielectric mode and when it is large this indicates that the fields are cavity-like.

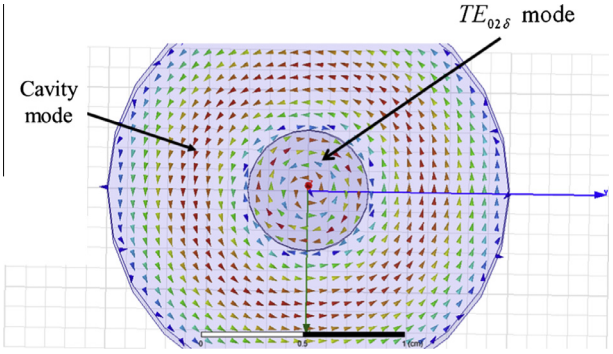

Fig. 7. A small cavity (2.0 cm × 2.0 cm) where the dielectric $TE_{02\delta}$ mode couples with the cavity TE_{011} mode.

By considering the coupling of the cavity with higher order modes, with the appropriate dimensions and frequency mentioned in the previous paragraph, it is possible to design a $TE_{011}/TE_{02\delta}$ probe that operates in the range of 19–23 GHz. The probe would also have a high filling factor due to the dielectric insert.

For any dimension, an approximate closed form expression for the electric field can be obtained. If the dielectric $TE_{01\delta}$ mode fields are calculated from Eq. (1) using the Cohn model [11], and the cavity electric field is calculated from Eq. (2), the electric field of the coupled system becomes,

$$E_\varphi = a_1 J_1(k_d r)\begin{cases}\cos(\beta z) & r \leqslant \frac{d_1}{2},\ |z| \leqslant \frac{l_1}{2} \\ e^{\frac{\alpha l}{2}}\cos\left(\frac{\beta l_1}{2}\right)e^{-\alpha|z|} & r < \frac{d_1}{2},\ |z| > \frac{l_1}{2}\end{cases} + a_2 J_1(k_c r)\cos\left(\frac{\pi z}{d_2}\right)$$

For *type I* resonators: β = 657 m^{-1}, α = 778 m^{-1} while for *type II:* β = *1293 m^{-1} and α = 2742 m^{-1}. The eigenvectors' components* a_1 *and* a_2 are easily determined from Eqs. (19) and (20).

4.4. Comparison between CMT and the LC model

Mett et al. have calculated the frequencies for the two modes of a DR in a cylindrical cavity using the LC model [7]. The cavity dimension was held constant $d_2 = l_2$ = 4.1598 cm and the DR was of *type II* where the diameter was allowed to vary from 1.3 mm to 2.1 mm. The frequencies of both the symmetric and anti-symmetric modes were determined by calculating the capacitances and inductances [7]. Excellent results were obtained when compared with HFSS® simulations.

These results have prompted us to compare the performance of the CMT and LC methods. In the current paper, the same circuit model in [7] is solved but, to avoid redundancy, a *type I* resonator is used instead of a *type II*. The cavity's diameter is allowed to change from 2.5 cm to 5.5 cm. Using HFSS® simulations as a reference, the errors in the frequencies of both the symmetric and anti-symmetric modes are calculated by the two techniques. Although the DRs considered by Mett et al. and the one used here have vastly different dielectric constants ($\varepsilon_r \approx 261$ and $\varepsilon_r \approx 30$ respectively) the LC model gives excellent results, over the range of 2.5 cm to 5.5 cm, with errors that are still below 5%. Coupled mode theory gives even better results in the same range with errors less than 1.5%.

In most practical cases the DR has a hole to accommodate the sample. The above results and discussion in this article will also

be valid in this case. In such a situation the frequency will slightly increase and the coupling coefficient will decrease due to the reduction of the overlap integral ζ. Because of the minor change in the DR frequency, its coupling with higher order modes is expected to be small.

5. Summary and conclusions

The frequencies and fields for a cavity with a high dielectric insert were studied using CMT. It was shown that the coupling coefficient is the normalized overlap integral. Physically, the dielectric insert affects the cavity by its polarization vector while the cavity injects energy into the dielectric mode through its surface current. Both effects were proven to be equal. General expressions for the eigenvalues, frequencies, eigenvectors and fields, both for the symmetric and anti-symmetric modes, were obtained.

There is excellent agreement between the frequencies obtained by CMT and HFSS®. While HFSS computations only give a numerical value for the frequency, the analytical expressions derived in this article by CMT give more insight. They show that the frequency is dependent on the coupling coefficient, κ. As the cavity diameter decreases, $\mathbf{E}_1^* \cdot \mathbf{E}_2$ and the overlap integral increase. This leads to a larger coupling coefficient. Consequently the frequencies differ from the uncoupled frequencies. In the case of the anti-symmetric mode the deviation of the frequency from the uncoupled structures could be as large as 500 MHz.

For different cavity dimensions, the expressions for the eigenvectors were used to study the fields' behavior of the coupled modes. It is shown that for large cavities ($\omega_2 \ll \omega_1$) the two modes tend to decouple. However for small cavities ($\omega_1 \ll \omega_2$), the coupling coefficient is large. From the eigenvectors point of view, the symmetric mode tends to be dominantly dielectric which means that the cavity acts as a shield. However, the anti-symmetric mode is always a mix of the two uncoupled modes. This observation was verified using the HFSS® eigenmodes solver. Here the coupling between the cavity's TE_{011} and the insert's $TE_{01\delta}$ modes were examined. It was observed that indeed the anti-symmetric mode has a dielectric insert component. The presence of the dielectric mode in the anti-symmetric mode implies that, in general, the signal to noise ratio of the spectrometer is improved.

Normally, the coupling between the cavity TE_{011} mode and other dielectric insert higher modes is usually small. However when the cavity's dimensions shrink to a level where the frequency of one of the higher order modes (for instance the dielectric $TE_{02\delta o}$ mode) gets closer to the cavity TE_{011} mode coupling occurs. This was also verified using HFSS® eigenmodes solver. By choosing the appropriate dimensions and frequency, it is possible to construct a $TE_{011}/TE_{02\delta}$ probe for a 19–23 GHz EPR spectrometer. Due to the dielectric insert, the probe would possess a high filling factor.

Coupled mode theory predicts that when the two resonators are degenerate ($\omega_1 = \omega_2$) the coupled modes are perfect combinations of the two uncoupled ones. Finite element simulations showed that the magnitude of the electric field along the cavity radius has two peaks. This verifies that the coupled modes are composed (linear combination) of the two uncoupled ones. Accordingly, the modes can be easily excited through an iris on the cavity walls. In addition, the filling factor has a lower value when compared to that of the dielectric in free space. This is because the electric field is delocalized in the cavity. Thus, when designing probes for electron paramagnetic spectroscopy, the coupling between the two structures should be taken into account.

Finally the frequencies of both the symmetric and anti-symmetric modes, calculated using CMT, are compared to those determined by the LC model [7]. The LC model shows that the error in frequency for moderately high epsilon inserts ($\varepsilon_r \approx 30$) is below 5% while CMT gives a maximum error bound of 1.5%.

From an experimental point of view, it is necessary to have a spectrometer with the highest sensitivity to detect dilute and weak samples. The sensitivity is directly related to a large resonator efficiency, Λ. This in turn is a function of the quality and filling factors [1,14,15]. In this article CMT is used to calculate analytical expressions for the magnetic fields. Compared to an empty CV, the fields of a probe consisting of a DR and a CV, are more localized in the vicinity of the sample which lead to a higher filling factor and consequently a higher sensitivity. From a different perspective, the CV component of the coupled modes provides an easy way to couple the probe to the microwave bridge via the CV iris. A shield can be considered as a cavity of smaller dimensions. It resonates at higher frequency and does not significantly affect the DR mode.

The findings and expressions in this article are general and can apply to any frequency range. They also apply whether the resonance is electronic or nuclear. For high frequency/high field EPR, the dielectric constant may significantly change with frequency. Hence, the solutions of the eigenvalue equation become more complicated.

The analysis here can be repeated for a LGR. However unlike a DR, the situation is slightly more complicated. An LGR has an inductive part represented by the loop. Thus a LGR may inductively couple with other TM modes (for example the TM111) mode which is degenerate with the TE_{011}.

Acknowledgments

SMM acknowledges the Natural Sciences and Engineering Research Council of Canada for financial support in the form of a discovery (operating) grant. SYN is grateful for the financial assistance from the University of New Brunswick in the form of pre-doctoral teaching and research assistantships. We would also like to acknowledge CMC Microsystems for the providing the HFSS suite of programs that facilitated this research.

References

[1] A. Blank, E. Stavitski, H. Levanon, F. Gubaydullin, Transparent miniature dielectric resonator for electron paramagnetic resonance experiments, Review of Scientific Instruments 74 (2003) 2853–2859.
[2] I. Golovina, I. Geifman, A. Belous, New ceramic EPR resonators with high dielectric permittivity, Journal of Magnetic Resonance 195 (2008) 52–59.
[3] S.M. Mattar, A.H. Emwas, A tuneable doubly stacked dielectric resonator housed in an intact TE102 cavity for electron paramagnetic resonance spectroscopy, Chemical Physics Letters 368 (2003) 724–731.
[4] Y.E. Nesmelov, J.T. Surek, D.D. Thomas, Enhanced EPR sensitivity from a ferroelectric cavity insert, Journal of Magnetic Resonance 153 (2001) 7–14.
[5] J.S. Colton, L.R. Wienkes, Resonant microwave cavity for 8.5–12 GHz optically detected electron spin resonance with simultaneous nuclear magnetic resonance, Review of Scientific Instruments 80 (2009). 035106-035106.
[6] S.M. Mattar, S.Y. Elnaggar, Analysis of two stacked cylindrical dielectric resonators in a TE102 microwave cavity for magnetic resonance spectroscopy, Journal of magnetic resonance (San Diego, CA: 1997) 209 (2011) 174–182.
[7] R.R. Mett, J.W. Sidabras, I.S. Golovina, J.S. Hyde, Dielectric microwave resonators in TE011 cavities for electron paramagnetic resonance spectroscopy, Review of Scientific Instruments 79 (2008) 94702.
[8] H. Haus, W.P. Huang, Coupled-mode theory, Proceedings of the IEEE 79 (1991) 1505–1518.
[9] I. Awai, New expressions for coupling coefficient between resonators, IECIE Transactions on Electronics E88-C (2005) 2295–2301.
[10] D.M. Pozar, Microwave Engineering, second ed., John Wiley and Sons, Hoboken, 2005.
[11] S.B. Cohn, Microwave bandpass filters containing high-Q dielectric resonators, Microwave Theory and Technique 16 (1968) 218–227.
[12] M. Popovic, C. Manolatou, M. Watts, Coupling-induced resonance frequency shifts in coupled dielectric multi-cavity filters, Optical Express 14 (2006) 1208–1222.
[13] B.W. Lennart Rade, Vector Identity Mathematics Handbook for Science and Engineering, fifth ed., Springer, Lund, Sweden, 2004.
[14] G. Feher, Sensitivity considerations in microwave paramagnetic resonance absorption techniques, Bell System Technical Journal (1957) 449–484.
[15] J.S. Hyde, W. Froncisz, T. Oles, Multipurpose loop-gap resonator, Journal of Magnetic Resonance 82 (1989) (1969) 223–230.